

# Optimum Docking of an Unmanned Underwater Vehicle for High Dexterity Manipulation

Panagiotis Sotiropoulos, Nikos Aspragathos, Fivos Andritsos

**Abstract**—A method for the determination of the optimum docking or hovering position of an Underwater Unmanned Vehicle is proposed for performing a desired intervention task with high dexterity. The optimization problem is formulated taken into account primarily the manipulator's dexterity in the area of intervention as well as the distance between the current position and the optimal one and the geometric constraints imposed by the environment. A Genetic Algorithm is designed and implemented to search for the best docking position. An underwater scenario with a UUV equipped with a 6 DOF manipulator is examined in order to verify the applicability of the proposed approach.

**Index Terms**— Optimization, Unmanned Underwater Vehicles, Dexterous Manipulation, Genetic Algorithms.

## I. INTRODUCTION

During the past few years underwater intervention operations have shaped a constantly growing field, mainly due to the demands of the hydrocarbon industry for the installation and maintenance of deepwater offshore sites. Search and recovery sector and institutes of underwater archaeology could also benefit from these developments. Since divers even with the use of Atmospheric Diving Suits can operate only up to 700 meters, deep water interventions are performed mainly by Unmanned Underwater Vehicles (UUVs) equipped with manipulators, such as the currently operating Remotely Operated Vehicles (ROVs). The emerging Intervention Autonomous Underwater Vehicles (IAUVs) could also provide a cost effective alternative in the near future. Some common underwater intervention tasks could be the manipulation of valves and switches on underwater facilities such as control panels on hydrocarbon underwater sites, the inspection and the maintenance, for example welding and cutting, on underwater structures and the object recovery and sampling from the sea bottom. In order to

perform an intervention the vehicle has to temporarily dock or hover near the desired target area. Currently, as far as it concerns ROVs, the selection of the docking pose is determined by the pilot usually based on his previous experience and intuition. Though, the pilot can not foresee the manipulator's kinematics as it reaches the working area and therefore an inadequate docking pose could be chosen. As a result a time consuming trial and error procedure is followed that could also be proven dangerous in critical situations. The determination of an appropriate docking position for the vehicle, through an automated process, that would provide high dexterity configurations of the manipulator for an intervention task would minimize the need for a re-docking. This would imply less time to perform a task, shorter mission and thus cost reduction.

In order to quantify the manipulator's dexterity and provide singularity free work poses, several measures have been proposed for land robotic manipulators. The dexterity measures for manipulator arms describe their ability to move freely in all directions of their workspace. Manipulability measures are based on the Jacobian matrix of the arm that relates the joint velocities of the motors with the end-effector velocities. These measures describe the ability of the manipulator to change the position and orientation of its end-effector given configuration. Any singular configurations of the arm could be also indicated by the value of the dexterity measure.

Yoshikawa [1] proposed dexterity indices based on the kinematic and the dynamic manipulability ellipsoid of the manipulator in order to provide a quantitative measure of a robot's ability for manipulation inside its workspace. Other indices have also been suggested such as the condition number of the Jacobian by Salisbury et al. [2] and the Manipulator Velocity Ratio (MVR) by Dubey et al. [3] as a measure of kinematic performance for the control of redundant manipulators. Aspragathos [4] proposed a globalised version of the Yoshikawa's manipulability index in order to determine the optimal location of a continuous path on the manipulator's workspace. Also an index for the velocity efficiency for a robot moving its end-effector along a path based on the minimum MVR along it was proposed by Aspragathos and Foussias in [5].

Regarding the determination of the optimum base pose of a robotic manipulator several works have been presented. The use of a genetic algorithm (GA) as the optimization method has been discussed in various papers. Mitsi et al. [6] proposed a method for determining the optimum robot base location

Manuscript received January 13, 2011. This work was sponsored by the FREESUBNET program, Contract number MTRN-CT-2006-036186

P. Sotiropoulos, is with the European Commission, Joint Research Centre, Ispra, VA 21027, Italy (Tel: 0039 0332785358 ; e-mail: panagiotis.sotiropoulos@jrc.ec.europa.eu).

N. Aspragathos, is with Mechanical Engineering and Aeronautics Department, University of Patras, Patras 26500, Greece (e-mail: asprag@mech.upatras.gr)

F. Andritsos, is with the European Commission, Joint Research Centre, Ispra, VA 21027, Italy (e-mail: fivos.andritsos@jrc.ec.europa.eu)

using a hybrid genetic algorithm. Tian et al. [7] used a GA to define the optimum base location for a two-link planar manipulator.

Even though the optimization of the robot's base location in order to maximize its dexterity, has been widely discussed for industrial applications, in underwater robotics relatively few researchers have dealt with this issue. Asokan has studied the optimum positioning of an underwater vehicle equipped with a manipulator to increase the efficiency on an underwater inspection task [8], noting that an inappropriate docking position would necessitate multiple re-dockings for the vehicle that would significantly increase the duration and the cost of the mission. For the special case of I-AUVs the avoidance of a re-docking would additionally mean energy savings that could lead to longer missions since energy capacity is limited. Moreover ensuring the dexterity of the manipulator arm from the vehicle's docking position to the tasks in hand prompts to faster manipulations and further time savings. A method to define such an appropriate docking pose as described above was proposed by Sotirtopoulos et al.[9] dealing only with the dexterity on the task point.

In this paper an algorithm that determines the optimum docking location for an UUV, equipped with a 6DOF robotic arm, performing an underwater intervention mission is presented. On the formulation of the objective function, a global dexterity index  $M_a$  for a predefined area of intervention, is considered as the measure of dexterity and it is based on the manipulability index  $w$  of the arm, as defined by Yoshikawa [1]. Though, Yoshikawa's manipulability index deals with a certain configuration of the arm, the area manipulability measure  $M_a$  is associated with a certain pose of the base with respect to a predefined task area assuring a minimum of dexterity inside this area. The distance between the UUV's current position and the proposed docking point, and the specific geometric restrictions imposed by the environment are also taken into account. A GA is implemented in order to solve the optimization problem and an underwater scenario that includes a grasping task is introduced for the demonstration of the method. The proposed algorithm provides a near-optimal docking pose for the vehicle. A number of test runs, in order to validate the applicability of the method, are presented in the Results section.

The paper is divided in the six following sections: *Introduction, Docking for Maximum Dexterity into an Area, Optimization Problem, Results, Conclusions and Future Work.*

## II. DOCKING FOR MAXIMUM DEXTERITY INTO AN AREA

The underwater scenario examined in this paper consists of a grasping task that should be performed by a hover-capable UUV after docking on a cement block that lays on the ocean bottom [10]. The block can be traced easily and the vehicle can navigate towards it either by acoustic or visual feedback control. On the top side of the block there is a hook that is to be grasped by the vehicle, Fig.1 and Fig.2. A depiction of the scenario appears in Fig. 3 when the UUV is approaching the block. The UUV is equipped with a 6-DOF elbow manipulator arm and is assumed that it can hover or dock on the determined optimal location. In order to dock firmly on

the block a common suction cup or another equivalent method could be used.

Navigation towards a target point and the acquisition of the relevant vehicle's pose can be performed using acoustic or vision feedback. Evans et al. [11], described an autonomous docking system (ADS) for the ALIVE AUV, that was using sonar and video based real-time 3D pose estimation to control the vehicle while it was navigating relative to the docking panel. Krupinski et al. [12] proposed a visual model-based pose estimation using an on-board camera and active markers on the subsea structure to guide the vehicle during its docking phase.

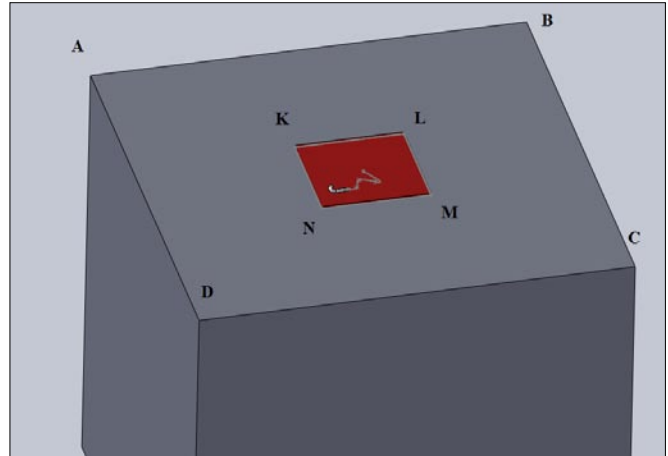


Figure 1: Task area on top of the cube

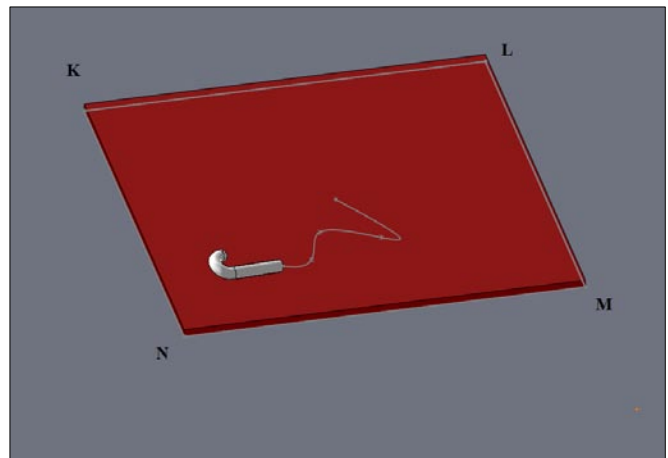


Figure 2: Hook inside task area

The described task is inspired by the deployment procedure of the DIFIS (Double Inverted Funnel for Intervention on Ship Wrecks) [10] dome and a near optimum docking position as described before should be determined.

In this work a method is proposed that could later be embedded in the control system of the vehicle. The algorithm receives as input the pose of the vehicle and the location of the target area. The manipulability measure is then calculated for the four outer corners  $K, L, M, N$  of a predefined area, around the centre of the upper surface of the cube, where the hook is expected to be, Fig.1 and Fig.2. Nevertheless, the hook could actually lay anywhere inside this area, due to water currents or initial misplacement. However, by guarantying a minimum

dexterity inside the task area the manipulator would still be able to operate with ease.

Utilizing a genetic algorithm the method returns a docking pose that assures high dexterity for the manipulator from this location to the task area.

### III. OPTIMIZATION PROBLEM

#### A. Formulating the objective function

Certain terms that are used in the present section are defined and demonstrated in Fig.3.

The *global coordinate system*  $G$  is located in the middle of the top face of the block and the *manipulator's coordinate system*  $B$  is located at its base on the front side of the UUV as it is shown in Fig. 3.

The *guessed optimal pose* ( ${}^G p$ ) indicates every candidate solution in the optimization problem and describes the manipulator's base. It is defined by  ${}^G p = [x \ y \ z]$  the position vector of the base of the manipulator in  $G$  and  $\psi$  the rotation angle about the  $z$ -axis of the frame  $G$ .

The *proposed docking point* ( ${}^G p_d$ ) is calculated according to each guessed optimal pose and refers to the vehicle's base where the suction cup is mounted. It is defined by  ${}^G p_d = [{}^G x_d \ {}^G y_d \ {}^G z_d]$  and indicated by the yellow star sign in Fig.3.

The *initial position of the manipulator's base* is given by  ${}^G p_{init} = [{}^G x_{init} \ {}^G y_{init} \ {}^G z_{init}]$  and the *initial position of the vehicle's base* is defined by  ${}^G p_i = [{}^G x_i \ {}^G y_i \ {}^G z_i]$  and is indicated by the red star sign in Fig.3.

The *task area* is shown on the top of the block and it is defined by four points  $K, L, M, N$  given by the position vectors  ${}^G p_{K0} = [x_{K0} \ y_{K0} \ z_{K0}]$ ,  ${}^G p_{L0} = [x_{L0} \ y_{L0} \ z_{L0}]$ ,  ${}^G p_{M0} = [x_{M0} \ y_{M0} \ z_{M0}]$  and  ${}^G p_{N0} = [x_{N0} \ y_{N0} \ z_{N0}]$ .

The UUV's base point, where the suction cup is mounted, is situated with respect to  $B$ , at  ${}^B p_{bp} = [{}^B x_{bp} \ {}^B y_{bp} \ {}^B z_{bp}]$ . It is demonstrated as the red disc on the bottom of the vehicle.

In the optimization process, every guessed optimal pose ( ${}^G p$ ) is evaluated according to the objective function until the best one is found. The red sphere on the tip of the manipulator represents the last 3R.

As stated before the criterion for the optimality of a certain docking pose is the area manipulability measure ( $M_a$ ). It is therefore calculated for every guessed optimal pose ( ${}^G p$ ) such as the one depicted in Fig. 3.

The  $M_a$  for each robot configuration is defined as the minimum manipulability measure in every control point ( $K, L, M, N$ ) of the task area. The area manipulability measure function  $M_a(w)$  is given by:

$$M_a(w) = \begin{cases} \min(\max(w_i^K), \max(w_i^L), \max(w_i^M), \max(w_i^N)) \\ , \text{ for } \theta_j^l < \theta_j < \theta_j^u, j = 1, \dots, 6, i = 1, \dots, 8 \\ 0, \text{ otherwise} \end{cases} \quad (1)$$

where  $w_i(\theta)$  is the manipulability measure for the  $i^{\text{th}}$  configuration of the manipulator, while reaching the outer corners of the task area  $K, L, M, N$ .

$\theta = [\theta_1 \dots \theta_j \dots \theta_6]$  are the joint angles derived by the inverse kinematics solution for the current guessed optimal pose  $[x, y, z, \psi]$ .  $\theta^l$  and  $\theta^u$  are the limits for every joint.

The manipulability measure for a configuration is derived through the solution of the inverse kinematics problem and the calculation of the Jacobian matrix.

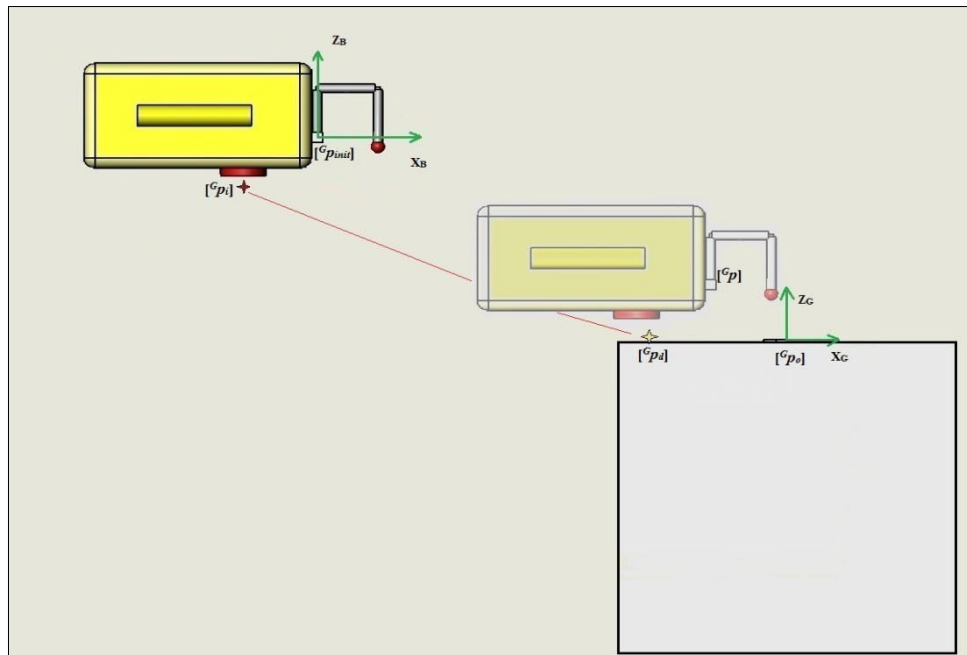


Figure 3: Side view of the vehicle and the block. Initial and proposed docking position

The inverse kinematics solution is based on the Paden-Kahan sub-problems [13]. The manipulability measure function is calculated according to:

$$w(\theta) = \sqrt{\det(J(\theta)J^T(\theta))} \quad (2)$$

where  $J(\theta)$  is the Jacobian matrix, and the vector  $\theta(x, y, z, \psi)$  is one of the possible joint configurations derived by the inverse kinematics solution for the considered pose.

It should be noted that for every single guessed optimal pose ( ${}^G p$ ) there can be up to eight different solutions of the inverse kinematic problem, thus eight manipulability measures. Thus, the maximum of these values for every control point is used for the calculation of the  $M_a$ .

On the formulation of the problem the area manipulability measure is not the only factor considered. Since various, symmetrical poses on the block may be equally good candidates, a distance factor would serve on selecting the less expensive one in terms of distance to be covered by the vehicle. Hence the distance between the initial position of the base of the vehicle ( ${}^G p_i$ ) and the proposed docking point ( ${}^G p_d$ ) is taken into account. The Euclidean distance between these two points is demonstrated as a red line in Fig. 2 and is given by:

$$D = \sqrt{({}^G x_i - {}^G x_d)^2 + ({}^G y_i - {}^G y_d)^2 + ({}^G z_i - {}^G z_d)^2} \quad (3)$$

${}^G p_i$  and  ${}^G p_d$  are derived by the following transformations:

$$\begin{bmatrix} {}^G p_i \\ 1 \end{bmatrix} = {}^G T_{O_B} \cdot \begin{bmatrix} {}^B p_{bp} \\ 1 \end{bmatrix} \quad (4)$$

$$\begin{bmatrix} {}^G p_d \\ 1 \end{bmatrix} = {}^G T_B \cdot \begin{bmatrix} {}^B p_{bp} \\ 1 \end{bmatrix} \quad (5)$$

where  ${}^G T_{O_B}$  is the homogeneous transformation matrix for the initial pose of the vehicle and  ${}^G T_B$  is the homogeneous transformation matrix for the guessed optimal pose ( ${}^G p$ ) given by:

$${}^G T_{O_B} = \begin{bmatrix} [R(\psi_{init})] & {}^G p_{init} \\ 0 & 0 & 0 & 1 \end{bmatrix} \quad (6)$$

$${}^G T_B = \begin{bmatrix} [R(\psi)] & {}^G p \\ 0 & 0 & 0 & 1 \end{bmatrix} \quad (7)$$

$R(\psi)$ : is the 3x3 rotation matrix that defines the rotation along the  $\psi$  angle referenced to the global coordinate system  $G$ .

$\psi_{init}$  is the initial angle of rotation of the vehicle about the  $z$ -axis of the frame  $G$ .

Summarizing, the optimization problem tackled here could be described as: *find the best docking position for the UUV given its initial pose and the target's position in order to ensure maximum manipulability in the desired area of intervention.*

The objective function for this problem is given below:

$$f_{obj} = a \cdot M_a(w) - b \cdot D(x, y, z) \quad (8)$$

where  $a, b$  are weighting factors used to transform the two terms of the objective function to comparable amounts, since they may take different magnitude of values.

Last, it has to be noted that the objective function is not continuous, due to the fact that for every single pose there exist multiple values for the area manipulability measure  $M_a(w)$  and in the case that the joint angle limits are exceeded, the area manipulability value turns to zero. In addition the solutions of the inverse kinematics problem are discrete and not continuous. Thus, the problem could not be solved with a simple gradient descent method and a GA is implemented to search for the optimum docking point.

### B. Optimization Based on GA

GA work in parallel to examine a number of initial points towards the search for the global minimum. In general, GA offer several advantages over other optimization methods, such as gradient methods, in the sense that they require only the objective function and not its derivative. They can find a near optimum solution even if the objective function is not continuous and they can perform robustly even in complex search spaces avoiding getting trapped in local minima. Also additional constraints could be easily specified inside the algorithm.

In this application, the field of values for the  $x, y, z$  coordinates is defined by the upper surface of the cube, adding a small margin  $d$  along the  $z$ -axis, where the final docking pose should be found. As a consequence the base point coordinates are bounded according to the following relations.

$$x_A \leq x \leq x_D \quad (9)$$

$$y_A \leq y \leq y_B \quad (10)$$

$$z_A \leq z \leq z_A + d \quad (11)$$

where  $d$  is the small margin above the cube's surface.

Though, further restrictions also occur since the docking pose should not be inside the task area.

$$x \geq x_N \text{ \& } x \leq x_K \quad (12)$$

$$y \geq y_L \text{ \& } y \leq y_K \quad (13)$$

From the above mentioned restrictions we can define a group  $Wd$  that all the possible solutions should lay in.

$$Wd = \left\{ \begin{array}{l} x: x_A \leq x \leq x_K \text{ \& } x_N \leq x \leq x_D, \\ y: y_A \leq y \leq y_K \text{ \& } y_L \leq y \leq y_B, \\ z: z_A \leq z \leq z_A + d \end{array} \right\} \quad (14)$$

Each individual that does not belong to  $Wd$  is given a penalty so as to be discarded in future generations. Thus the fitness function of the GA becomes:

$$f_{fit} = \begin{cases} a \cdot M_a(w) - b \cdot D(x, y, z), \forall {}^G p \in Wd \\ 0, \text{ otherwise} \end{cases} \quad (15)$$

In this particular problem each chromosome of the GA consists of the  $x, y$  and  $z$  coordinates for its position and  $\psi$

Yaw angle for its orientation and it is represented as a binary chromosome of the form:

|          |          |          |         |
|----------|----------|----------|---------|
| <i>x</i> | <i>y</i> | <i>z</i> | $\psi$  |
| 10...11  | 10...11  | 10...11  | 01...11 |

The length of every part of the chromosome depends on the range of field of values of each variable and the selected accuracy. As in this specific problem the GA does not run the risk of getting trapped into local minima a modified crossover probability is assigned in each individual in order to favour the fittest ones. In addition during the execution of the algorithm the mutation and the crossover probability are being reduced as better solutions are achieved and the number of generations grows. The algorithm stops when the maximum number of generations is reached or the value of the fitness function as converged. There exists also another termination criterion that is, if the best value of the fitness function has not changed for 50 generations the algorithm stops providing the best pose found so far.

IV. RESULTS

The cement block's and the UUV's dimensions in meters, along the *x*, *y* and *z* axis are, 2x2x2 (m) and 1.5x1.2x1 (m), respectively. The task area's dimensions are 0.4x0.4 (m) located on the centre of the upper surface of the cube. The manipulator is a 6R with a spherical joint for the last three 3R. The lengths of the links are  $l_0=0.1m$ ,  $l_1=l_2=0.4m$ . The joints' angle limits are given in Table 1.

Table 1: Angle limits

| Lower limit | Angle      | Upper limit |
|-------------|------------|-------------|
| -2.8        | $\theta_1$ | 2.8         |
| -2.35       | $\theta_2$ | 2.35        |
| -2.35       | $\theta_3$ | 2.35        |
| -4.6        | $\theta_4$ | 4.6         |
| -4.6        | $\theta_5$ | 4.6         |
| -2.6        | $\theta_6$ | 2.6         |

A scheme of the manipulator on its zero angle configuration is demonstrated in Fig.4 below using Matlab's Robotic Toolbox [14]:

The vehicle's initial position is given by  ${}^G p_{init}=[-2 \ -2 \ 2]$  and the vehicle's base position relative to *B* is given by  ${}^B p_{bp}=[-0.3 \ 0 \ -0.2]$ .

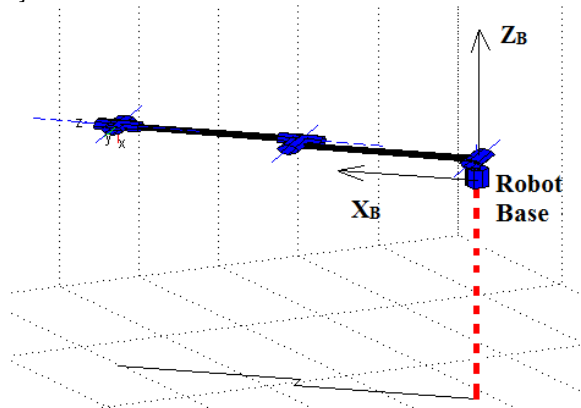


Figure 4: Manipulator at zero angle configuration

After several executions of the GA, the initial values for the crossover and mutation probabilities and the value of the Population and generation size have been set to the following:

Table 2: GA settings

| Crossover Probability | Mutation Probability | Population Size | Generations |
|-----------------------|----------------------|-----------------|-------------|
| 0.20                  | 0.08                 | 60              | 500         |

The results obtained from each run are a near optimum docking pose, its fitness function value and the maximum acquired area manipulability measure. The results for seven consecutive runs are demonstrated in Table 3.

After the acquisition of the poses, post process calculations are made to acquire the four configurations for the manipulator in order to reach the task area control points that are demonstrated in Table 4.

Table 3: Results

|   | <i>x</i> | <i>y</i> | <i>z</i> | $\psi$ | Fitness value | Ma    |
|---|----------|----------|----------|--------|---------------|-------|
| 1 | -0.32    | -0.36    | 0.24     | 0.79   | 2.95          | 0.181 |
| 2 | -0.49    | -0.32    | 0.23     | 0.83   | 2.34          | 0.137 |
| 3 | -0.28    | -0.46    | 0.24     | 0.77   | 2.55          | 0.151 |
| 4 | -0.36    | -0.38    | 0.22     | 0.74   | 2.26          | 0.134 |
| 5 | -0.36    | -0.37    | 0.24     | 0.78   | 2.38          | 0.141 |
| 6 | -0.31    | -0.39    | 0.20     | 0.79   | 2.64          | 0.164 |
| 7 | -0.31    | -0.38    | 0.21     | 0.73   | 2.84          | 0.177 |

The configurations of the manipulator for the first run are depicted in Fig.5, Fig.6, Fig.7 and Fig.8. For this pose the maximum manipulability measure  $w_{max}$  across the task area is plotted and illustrated in Fig.9, where it can be observed that it remains in high values in the greater part of the surface.

$$w_{max} = \max(w_{x,y}^i), \text{ for } i = 1, \dots, 8, x, y \in [-0.2, 0.2] \quad (16)$$

Table 4: Configurations

|   | $\theta_1$ | $\theta_2$ | $\theta_3$ | $\theta_4$ | $\theta_5$ | $\theta_6$ |
|---|------------|------------|------------|------------|------------|------------|
| K | 2.724      | 2.241      | 2.185      | -1.7e-15   | -2.567     | 2.467      |
| L | 0.657      | 0.137      | -1.348     | 0          | 0.359      | 1.695      |
| M | 0.098      | -0.608     | 0.377      | 9.45e-17   | 1.802      | 0.888      |
| N | -0.340     | -1.279     | 1.438      | -6.6e-17   | 1.412      | -0.391     |

From Table 4 it can also be observed that the manipulator's angles remain away from their limits for the three control points *L*, *M*, *N*, while for the point *K* the first three angles are near their limits. This is the reason why in the plot of Fig.9 it appears a quite small area with zero manipulability, the fact that the manipulator reaches its inner workspace limits. This could imply that the four control points of the task area, on which the manipulability measure is calculated, might not be sufficient and further control points should be introduced. Nevertheless, the introduction of even more control points would make the algorithm run slower.

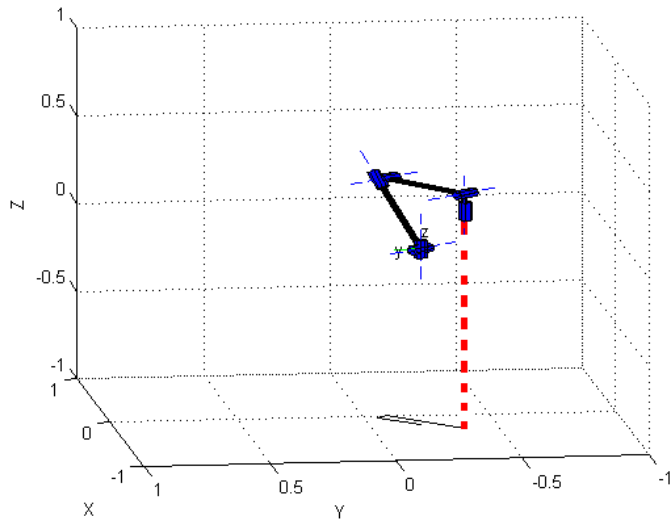


Figure 5: Configuration on control point K

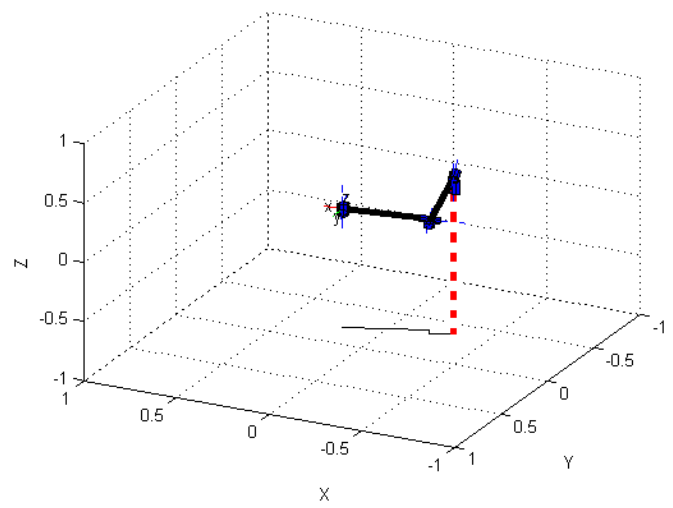


Figure 8: Configuration on control point N

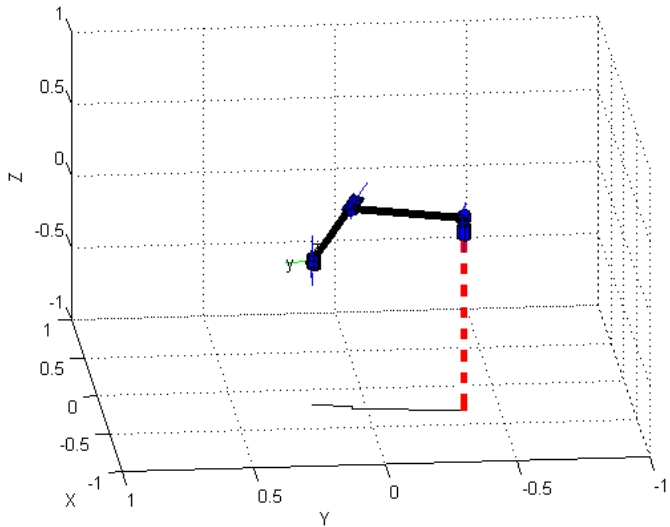


Figure 6: Configuration on control point L

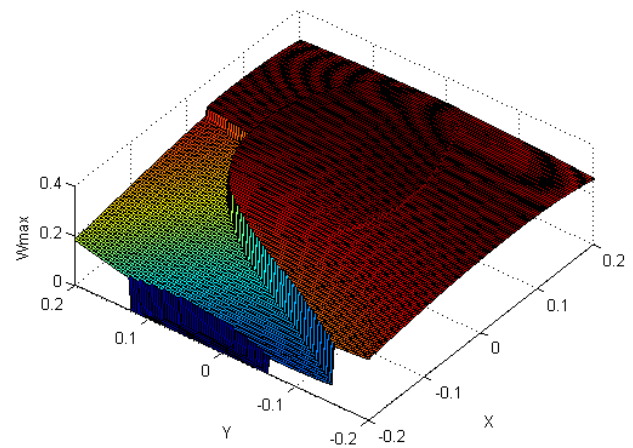


Figure 9:  $w_{max}$  on the task area

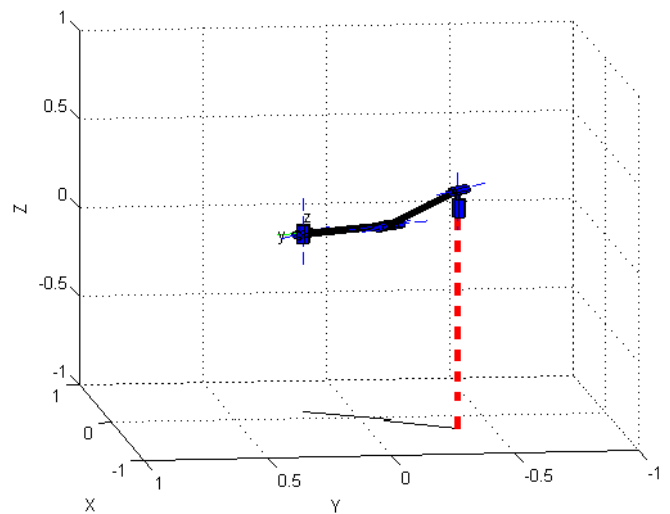


Figure 7: Configuration on control point M

Though, it could be easily demonstrated that on the same quarter of the upper surface of the cube there can exist also inappropriate poses for the manipulator's base, like the:

| $x$    | $y$    | $z$   | $\psi$ |
|--------|--------|-------|--------|
| -0.491 | -0.464 | 0.213 | 0.83   |

The plot of the maximum manipulability  $w_{max}$  across the task area also for this pose is demonstrated in Fig.10 below. It can be easily observed that the manipulability measure is zero for a significant part of the task surface. This implies that manipulations of any kind on this part of the surface would be rather impossible and a re-docking of the vehicle would be necessary.

Nevertheless the GA in every run manages to avoid similar cases and to provide high dexterity poses for the manipulator's base.

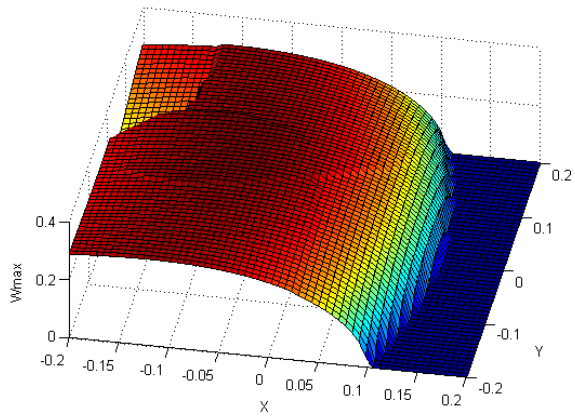


Figure 10:  $w_{\max}$  plot for an ill-placed docking pose

It should be also noted that all the proposed docking poses lay on the same quarter of the upper surface of the cube, since it is the nearest to the predefined initial position. Also all the selected poses face the target, so as the cameras of the vehicle can observe easier the task scene. An indicative representation of the docking pose with respect to the cube is demonstrated in Fig 11. The yellow point in the figure represents the docking point of the vehicle. The red one represents the manipulator's base, while the blue one is a projection of the manipulator's base on the cube's surface.

## V. CONCLUSION

In this paper a method was proposed to determine the optimum docking position of an UUV equipped with a 6 DOF manipulator for an underwater intervention task. The GA implemented here received as an input the initial vehicle's position and the position of the block and returned a near optimum docking position on the block. The determined docking position assured high value of the manipulability measure on the task region while it was staying inside the margins set in order to dock on the top of the block. The proposed algorithm could be embedded in a UUV mission control system when intervention tasks are to be performed.

In this particular case the docking case examined imposed the suppression of the roll and pitch angles, since the vehicle had to dock on the top of the block with its bottom side. The algorithm can easily be modified to deal with different cases were the vehicle has to dock on a vertical surface. In the case of a hover capable vehicle the docking position could be calculated in the same way simply by extending the chromosome and taking into account the Roll and Pitch angles.

## VI. FUTURE WORK

Further work will follow on the motion planning for the manipulator in order to acquire collision free configurations. Moreover further control points should be introduced while calculating the minimum manipulability measure of the task area in order to eliminate the risk of having even small areas with low manipulability inside the area from the selected docking pose.

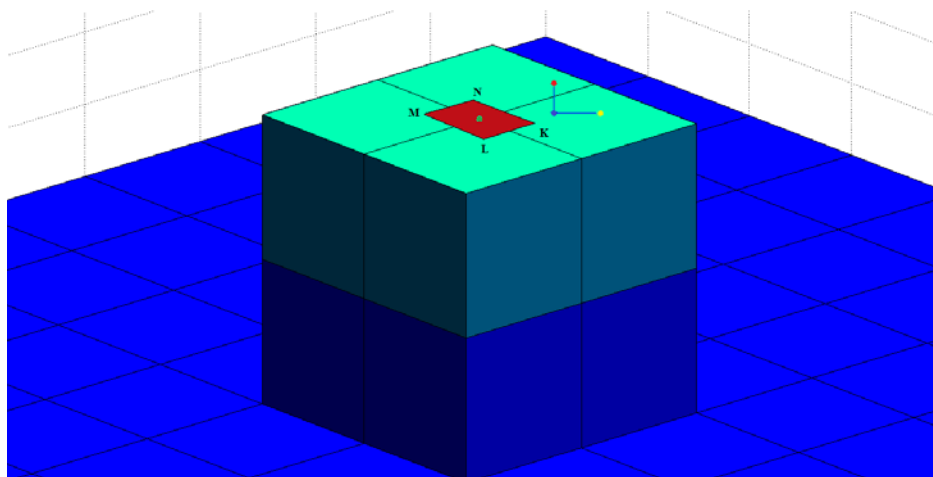


Figure 11: Final docking pose

APPENDIX

In this appendix the selected poses for the manipulator's configuration on the four control points are demonstrated in detail. The orientation of the end effector could also be observed.

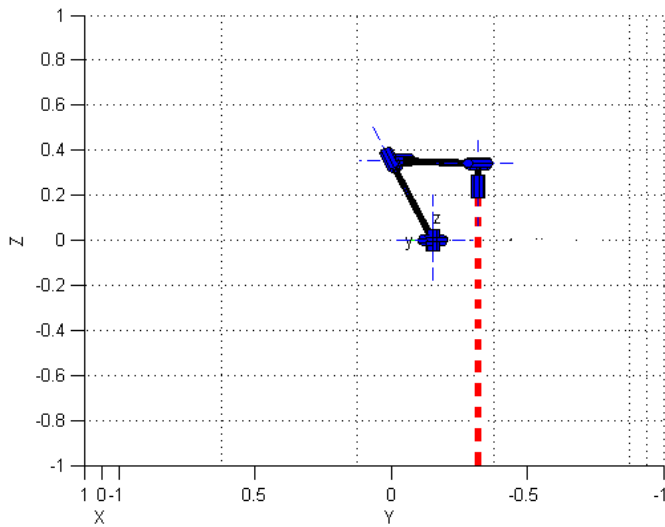


Figure 12: Side view of configuration on control point K

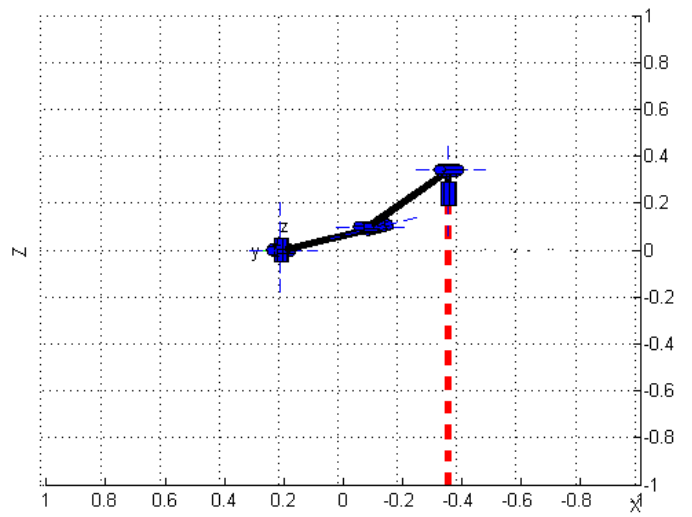


Figure 14: Side view of configuration on control point M

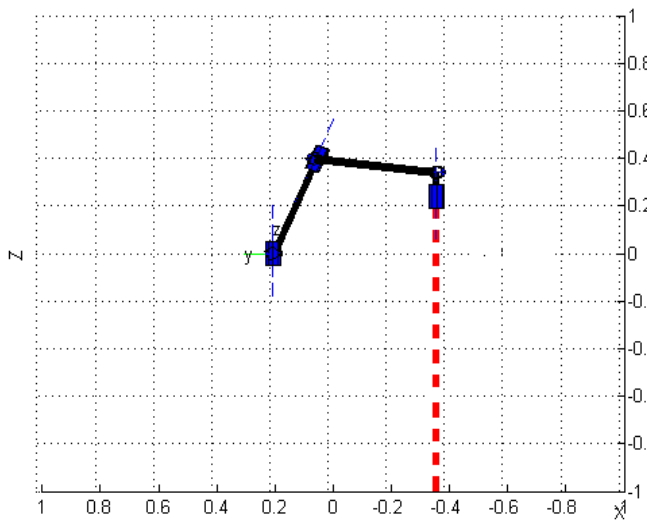


Figure 13: Side view of configuration on control point L

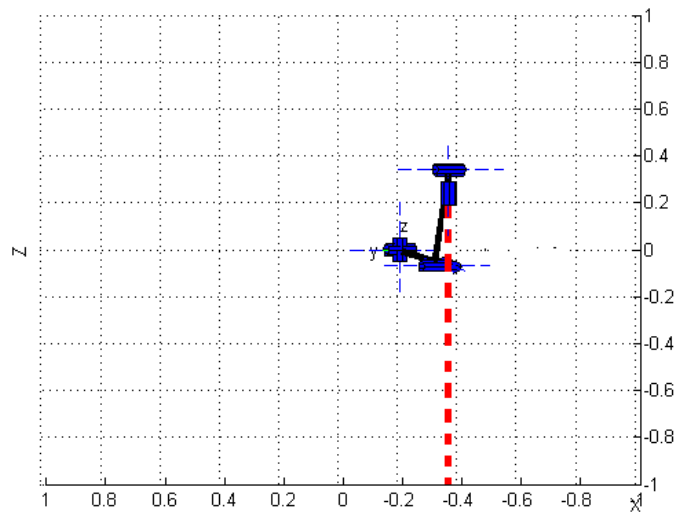


Figure 15: Side view of configuration on control point N

## REFERENCES

- [1] T. Yoshikawa, Ed., *Foundations of Robotics*. Cambridge Massachusetts: The MIT Press, 1990, p.^pp. Pages.
- [2] J. K. Salisbury and J. J. Craig, "Articulated Hands," *The International Journal of Robotics Research*, vol. 1, pp. 4-17, March 1, 1982 1982.
- [3] R. Dubey and J. Y. S. Luh, "Redundant robot control using task based performance measures," *Journal of Robotic Systems*, vol. 5, pp. 409-432, 1988.
- [4] N. A. Aspragathos, "Optimal Location of Path Following Tasks in the Workspace of a Manipulator using Genetic Algorithms," in *ARK'96*, Portoroz, Slovenia, 1996, pp. 179-188.
- [5] N. A. Aspragathos and S. Foussias, "Optimal location of a robot path when considering velocity performance," *Robotica*, vol. 20, pp. 139-147, 2002.
- [6] S. Mitsi, *et al.*, "Determination of optimum robot base location considering discrete end-effector positions by means of hybrid genetic algorithm," *Robotics and Computer-Integrated Manufacturing*, vol. 24, pp. 50-59, 2008.
- [7] L. Tian and C. Collins, "Optimal placement of a two-link planar manipulator using a genetic algorithm," *Robotica*, vol. 23, pp. 169-176, 2005.
- [8] T. Asokan, *et al.*, "Optimum positioning of an underwater intervention robot to maximise workspace manipulability," *Mechatronics*, vol. 15, pp. 747-766, 2005.
- [9] P. Sotiropoulos, *et al.*, "Determination of the optimum docking position of an underwater unmanned vehicle using a genetic algorithm," *Lecture Notes in Engineering and Computer Science: Proceedings of The World Congress on Engineering and Computer Science 2010, WCECS 2010, 20-22 October, 2010, San Francisco, USA*, pp.340-345.
- [10] DIFIS. *DIFIS project web site*. Available: <http://www.ifremer.fr/difis/>
- [11] J. Evans, *et al.*, "Autonomous docking for Intervention-AUVs using sonar and video-based real-time 3D pose estimation," in *OCEANS 2003. Proceedings*, 2003, pp. 2201-2210 Vol.4.
- [12] S. Krupinski, *et al.*, "Investigation of autonomous docking strategies for robotic operation on intervention panels," in *OCEANS 2008*, 2008, pp. 1-10.
- [13] R. Murray, *et al.*, *A Mathematical Introduction to Robotic Manipulation*: CRC, 1994.
- [14] P. I. Corke, "A robotics toolbox for MATLAB," *IEEE Robotics and Automation Magazine*, vol. 3, pp. 24-32, 1996.